International Journal of Sciences and Techniques of Automatic control & computer engineering
IJ-STA, Volume 5, N° 2, December 2011, pp. 1660–1677.

Ant Colony Optimization Based Fuzzy Sliding Mode Controller for the Twin Rotor MIMO system

F. Allouani[1], D. Boukhetala[1] and F. Boudjema[2]

[1]Department of Engineering Sciences, University Centre of Khenchela, Algeria,
allouani_fouad@yahoo.fr
[2]Laboratoire de commande des processus, Automatic Control Department,
Ecole Nationale Polytechnique, Algiers, Algeria,

Abstract. *The ant colony optimization (ACO) algorithm is an evolutionary computational technique based on the behavior of a set of ants that communicate through the deposit of pheromone. It involves a node choice probability which is a function of pheromone strength and inter-node distance to construct a path through a node-arc graph. The algorithm allows fast near optimal solutions to be found compared to other stochastic methods. In this paper, a novel approach for angel positions control of a Twin Rotor Multi input–multi output System (TRMS) by means of a sliding mode controller (SMC), fuzzy logic controller (FLC) and ACO is investigated. For decreasing the chattering problem of the SMC, a FLC is used to replace the discontinuity in the sign function of the reaching law in the SMC. For selecting sliding surface constants and FLC input/output membership function parameters, the basic ACO algorithm is employed to search these parameters. To verify the feasibility and robustness of the control method, simulation results from a TRMS with the designed controller are given as an illustration. Furthermore, the performance comparisons with the Proportional Integral Differential (PID) controller tuned using the same method are provided to show that the control method has better performance in the aspect of tracking error and control signals energy.*

Keywords. *Fuzzy control, sliding mode, ant colony optimization, TRMS.*

1. Introduction

Conventional control laws such as PID are successful in the case of linear systems with constant parameters. Contrariwise, in the case of nonlinear systems or with systems having non constant parameters, these laws can be inadequate because they are not robust. Variable-structure controller (VSC) inherently a non linear control technique provides an efficient solution to these problems. The main feature of this technique is that their control law is changing in a discontinuous way. The switching

This paper was recommended for publication in revised form by the editor Staff.
Edition: CPU of Tunis, Tunisia, ISSN: 1737-7749

control mechanism is performed according to some state variables, used to create a "variety" or "surface" so-called sliding surface where its goal is to force the dynamic of system to correspond with that defined by the sliding surface equation. When the state of the system is maintained in this surface, the system is said in the sliding regime, where it remains insensitive to parameter variations and external disturbances.

This sliding mode is often described as ideal, because it requires for existing an infinitely high switching frequency. On the other hand, any real control system includes imperfections such as: delays, hysteresis requires a finite switching frequency. Then, the trajectory of state oscillates in a neighborhood of the sliding surface that generates the undesirable chattering phenomenon. In this paper a FLC is used to replace the discontinuity in the sign function of the reaching law in the SMC for decreases the chattering problem. This method is appeared to be a good idea and many researchers have published various control scheme base on this idea [1], [2], [3]. However, Selection a group of suitable parameters to the predefined sliding surface and membership functions for the FLC is very important, which are relative to the dynamic performance of the control system.

Ant colony optimization (ACO) is a population based algorithm proposed by M Dorigo and colleagues [4] as a novel nature inspired meta-heuristic for the solution of hard combinatorial optimization (CO) problems. It has been inspired by the foraging swarming behavior of real ant colonies, which have been observed capable of finding the shortest (optimal) path between their nest and a food source, the virtual ants in ACO aim at jointly finding optimal paths in a given search space. This is attributed to the fact that ants communicate via pheromone that they use in variable quantities to mark their trails. An ant has a tendency to choose a specific path with the greatest amount of pheromone. However, the pheromone trail evaporates over time, i.e., it loses intensity if no more pheromone is laid down by other ants. So, that over time the intensity of the pheromone trail in the shortest path increases and thus this trail traversed more quickly and attracts more and more ants. This characteristic of real ant colonies is exploited in artificial ant colonies in order to solve CO problems.

In this paper, a decentralized fuzzy sliding mode controller (DFSMC) is designed to position the yaw and pitch angles of a TRMS based on the kinematics of this system and the basic ACO algorithm which is utilized to optimize the FLCs membership function parameters and the sliding surface constants parameters of the controller. To verify the feasibility and robustness of the control method, simulation results from the TRMS with the controller designed by the presented method are given as an illustration. The reminder of this paper is organized as follows. In Section 2, the dynamics of the TRMS is described. The ACO-tuning method for the DFSMC is designed in Section 3. Section 4 presents the simulation results to demonstrate the effectiveness of the control method. Finally, conclusions are drawn in Section 5.

2. The twin rotor MIMO system

The TRMS is a laboratory set-up developed by Feedback Instruments Limited for control experiments [5]. As shown in Fig. 1, this system is characterized by a complex

highly nonlinear dynamics, where some states are inaccessible for measurements, and hence this set-up can be considered as a challenging engineering problem [6], [7]. The TRMS consists of a beam pivoted on its base in such a way that it can rotate freely in both horizontal and vertical planes. At the two ends of the beam, there are two rotors (the main and tail rotors) driven by direct current (DC) motors. A counterbalance arm with a weight is fixed at the pivot point of the beam (see Fig. 1).

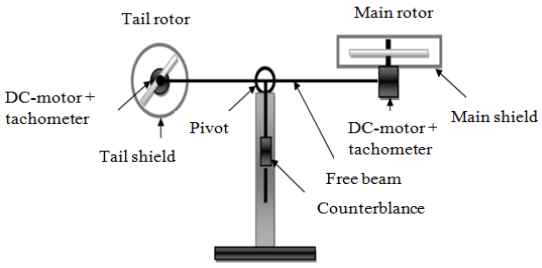

Fig. 1. Twin Rotor MIMO System

The control objective is to set the beam of the TRMS at the desired positions (the pitch angle α_v and the yaw angle α_h) quickly and accurately. All the meanings of the TRMS parameters are given in the following Nomenclature [5]:

- $F_{h/v}(\omega_{h/v})$: Two nonlinear characteristics determining dependence of propeller thrust on DC motor rotational speeds $\omega_{h/v}$,
- $P_{h/v}(u_{h/v})$: Two nonlinear input characteristics determining dependence of tail/main DC motor rotational speed $\omega_{h/v}$ on tail/main input voltage $u_{hh/vv}$,
- l_t: Length of the tail part of the beam (m),
- l_m: Length of main part of the beam (m),
- $\alpha_{h/v}$: Horizontal/vertical position of the beam (rad),
- J_v: The sum of moments of inertia relative to the horizontal axis (kg·m^2),
- $J_h(\alpha_{v0})$: Moment of inertia about vertical axis (kg·m^2),
- $k_{h/v}$: Positive constants,
- T_{tr},T_{mr} : Time constants of tail/main rotors,
- $k_{tr/mr}$: Tail/main motor propeller positive constants,
- $J_{tr/mr}$: Moment of inertia in DC-motor tail/main propeller subsystem (kg·m^2).
- A,B,C: Constants calculated according to the TRMS dynamic model parameters.

The mathematical model of the remaining parts of the system in vertical plane is described by (1) to (3) (see [5]). This model is derived from the coupled model (see [4]) by setting the azimuth angle α_h=0 (rad) and putting u_h=0 (v). We choose the following state vector $X_v=[x_1\ x_2\ x_3]^T=[\alpha_v\ s_v\ u_{vv}]$. So, the state space of the one degree of freedom (1-DOF) model of the Vertical Subsystem (VS) of the TRMS is described as follow:

$$\frac{dx_1}{dt} = \frac{x_2}{J_v} \ . \tag{1}$$

$$\frac{dx_2}{dt} = I_m F_v\left(P_v\left(x_3\right)\right) - k_v \frac{x_2}{J_v} + g\left(\left(A-B\right)\right)\cos\left(x_1\right) - Csin(x_1)) \ . \tag{2}$$

$$\frac{dx_3}{dt} = \frac{1}{T_{mr}}\left(-x_3 + k_{mr}u_v\right) . \tag{3}$$

In the same way as the 1-DOF model of the VS, the 1-DOF model of the Horizontal Subsystem (HS) is derived by setting the pitch $\alpha_v = \alpha_{v0}$ angle and putting u_v=0 (v). Our choice for the state vector is $X_h=[x_1\ x_2\ x_3]^T=[\alpha_h\ s_h\ u_{hh}]$. So, the state space of the 1-DOF model of the HS of the TRMS is as follow (see [5]):

$$\frac{dx_1}{dt} = \frac{x_2}{J_h(\alpha_{v0})} \ . \tag{4}$$

$$\frac{dx_2}{dt} = I_t F_h\left(P_h\left(x_3\right)\right)\cos\left(\alpha_{v0}\right) - k_h\left[\frac{x_2}{J_h(\alpha_{v0})}\right] . \tag{5}$$

$$\frac{dx_3}{dt} = \frac{1}{T_{tr}}\left(-x_3 + k_{tr}u_h\right) . \tag{6}$$

3. Design of ACO-based Fuzzy Sliding Mode Controller for the TRMS

3.1. Design of DFSMC for the TRMS

SMC is a method derived from Variable Structure Control (VSC) which was originally studied by [8]. The controller designed using this technique is particularly appealing due to its ability to deal with nonlinear systems and time-varying systems [3], [9]. SMC proved their high accuracy and robustness with respect to various internal and external disturbances. The basic idea of this method is to force the system, after a finite time reaching phase, to a sliding surface *s(x,t)* containing the system operating point and defined to represent a desired global behavior for instance stability and tracking performance.

The $s(x,t)$ selected in this work is presented by [10]:

$$s(x,t)=\left(\frac{d}{dt}+\lambda\right)^{n-1}e(t). \quad (7)$$

Where λ is a positive constant.

It is clear from (7) that keeping the states of the system on the sliding surface will guarantee the tracking error vector *e* asymptotically reaching to zero. The corresponding sliding condition [10] is:

$$\frac{dV(t)}{dt}=\frac{1}{2}\frac{d}{dt}s^2(x,t)=s(x,t)\dot{s}(x,t)<0. \quad (8)$$

Where *V(t)* indicates the Lyapunov function defined as:

$$V(t)=\frac{1}{2}s^2(x,t). \quad (9)$$

The general control structure that satisfies the stability condition of the sliding motion can be written as [11]:

$$u=u_{eqv}-ksgn(s). \quad (10)$$

Where u_{eqv} is called the equivalent control law that is derived by setting $ds/dt=0$ and *k* is a positive constant. As the relative degree is $n=3$ for the two subsystems we obtain the following two sliding surfaces:

$$s_v(x,t)=\lambda_v^2 e_v+2\lambda_v\frac{de_v}{dt}+\frac{d^2e_v}{dt^2}. \quad (11)$$

$$s_h(x,t)=\lambda_h^2 e_h+2\lambda_h\frac{de_h}{dt}+\frac{d^2e_h}{dt^2}. \quad (12)$$

Where, $e_v(t)$ and $e_h(t)$ is the pitch angle error and the yaw angle error respectively. In general case, when the closed loop system is in the sliding mode, it satisfies the condition $ds(x,t)/dt=0$ and then the equivalent control law is obtained. First, we compute the equivalent control law $u_{eqv\,v}$ for the VS as follows. Then, we have:

$$\frac{ds_v(x,t)}{dt}=\lambda_v^2\frac{de_v}{dt}+2\lambda_v\frac{d^2e_v}{dt^2}+\frac{d^3x_1}{dt^3}-\frac{d^3x_{1d}}{dt^3}. \quad (13)$$

Because $e_v(t)=\alpha_v(t)-\alpha_{vd}(t)=x_1-x_{1d}$ where $\alpha_{vd}(t)$ is the desired position of the beam in the vertical plane, the (13) becomes:

$$\frac{ds_v(x,t)}{dt}=\lambda_v^2\frac{de_v}{dt}+2\lambda_v\frac{d^2e_v}{dt^2}+\frac{d^3x_1}{dt^3}-\frac{d^3x_{1d}}{dt^3}. \quad (14)$$

We replace the two terms:
$F_v(P_v(x_3))$ and $g((A-B))\cos(x_1)-C\sin(x_1))$ in (2) by the following expressions:

$F_v(P_v(x_3))=f_v(x_3)$ and $g((A–B))cos(x_1)–Csin(x_1))=g_v(x_1)$ and we use the condition $ds_v(x,t)/dt=0$ we can obtain the value of the equivalent control law $u_{eqv\,v}$ for the VS:

$$u_{eqvv}=\frac{-1}{\frac{I_m k_{mr}}{J_v T_{mr}}\frac{df_v(x_3)}{dx_3}}[\lambda_v^2\frac{de_v}{dt}+2\lambda_v\frac{d^2e_v}{dt^2}-\frac{d^3x_{1d}}{dt^3}-\frac{I_m}{J_v T_{mr}}\frac{df_v(x_3)}{dx_3}x_3-\frac{k_v}{J_v^2}\frac{dx_2}{dt}+\frac{dg_v(x_1)}{dx_3}\frac{x_2}{J_v^2}] \quad (\mathbf{15})$$

Now, we attempt to calculate the equivalent control law $u_{eqv\,h}$ for the HS. So, we have:

$$\frac{ds_h(x,t)}{dt}=\lambda_h^2\frac{de_h}{dt}+2\lambda_h\frac{d^2e_h}{dt^2}+\frac{d^3e_h}{dt^3} \quad . \quad (\mathbf{15})$$

We have $e_h(t)=\alpha_h(t)-\alpha_{hd}(t)=x_1-x_{1d}$ where $\alpha_{hd}(t)$ is the desired position of the beam in the horizontal plane, the (16) becomes:

$$\frac{ds_h(x,t)}{dt}=\lambda_h^2\frac{de_h}{dt}+2\lambda_h\frac{d^2e_h}{dt^2}+\frac{d^3x_1}{dt^3}-\frac{d^3x_{1d}}{dt^3} \quad . \quad (\mathbf{16})$$

As before with the VS and by setting $ds_h(x,t)/dt=0$, we can obtain the value of the equivalent control law $u_{eqv\,h}$ for the HS:

$$u_{eqvh}=\frac{-1}{\frac{I_t k_{tr}cos(\alpha_{v0})}{J_h(\alpha_{v0})T_{tr}}\frac{df_h(x_3)}{dx_3}}[\lambda_h^2\frac{de_h}{dt}+2\lambda_h\frac{d^2e_h}{dt^2}-.\frac{d^3x_{1d}}{dt^3}-\frac{I_t cos(\alpha_{v0})}{J_h(\alpha_{v0})T_{tr}}\times\frac{df_h(x_3)}{dx_3}x_3-\frac{k_h}{J_h^2(\alpha_{v0})}\frac{dx_2}{dt}] \quad (\mathbf{17})$$

Where: $F_h\,(P_h(x_3))=f_h(x_3)$,
The SMC from (14) can be obtained for the VS using the following control law:

$$u_v=u_{eqv\,v}-k_v sgn(s_v) \quad . \quad (\mathbf{19})$$

Where k_v is the positive switch gain and $sgn(s_v)$ is the sign function.
Using (19) in (14), results:

$$\dot{s}_v(x,t)=-k_v sgn(s_v) \quad . \quad (\mathbf{20})$$

Then, the condition in (8) is verified and the VS states are now approaching to the hyperplane, and the error $e_v(t)$ asymptotically reduces to zero once the system state reaches $s_v(x,t)=0$, and $\alpha_v(t)$ will asymptotically converges to its desired value. Moreover, the SMC guarantees the asymptotic convergence of the output to its desired value. The same procedure design is used with the HS. Therefore, using the

control law given in the following equation allows to verify the condition mentioned in (8).

$$u_h = u_{eqv\,h} - k_h sgn\left(s_h\right) \tag{21}$$

If the control laws u_v and u_h are chosen as (19) and (21), chattering phenomena will occur after the first time state hits the sliding surface. In order to overcome this problem, a FLC is suggested and applied to construct the switching control law in (19) and (21).

The main advantage of the FLC is its heuristic design procedure and it is a model-free approach. The SMC approach has important advantages such as fast response, less sensitive to uncertainties and has no need for online identification of plant parameters. The combination of FLC strategy and SMC method becomes a feasible approach to preserve the advantages of these two approaches. A fuzzy sliding surface is introduced to develop a SMC. The IF-THEN rules base of DFSMC is designed as [12]:

R^{1}: If $s_{h/v}$ is **Negative Big**, then $u_{Fuzzy\ h/v}$ is **Positive Big**.
R^{2}: If $s_{h/v}$ is **Negative Small**, then $u_{Fuzzy\ h/v}$ is **Positive Small**.
R^{3}: If $s_{h/v}$ is **Zero**, then $u_{Fuzzy\ h/v}$ is **Zero**.
R^{4}: If $s_{h/v}$ is **Positive Small**, then $u_{Fuzzy\ h/v}$ is **Negative Small**.
R^{5}: If $s_{h/v}$ is **Positive Big**, then $u_{Fuzzy\ h/v}$ is **Negative Big**.

Where; Negative Big (NB), Negative Small (NS), Zero (ZO), Positive Small (PS), Positive Big (PB) are labels of fuzzy sets. The membership functions of these linguistic labels for the terms $s_{h/v}$ and $u_{Fuzzy\ h/v}$ are shown in Fig. 2 (a) and Fig. 2 (b) respectively.

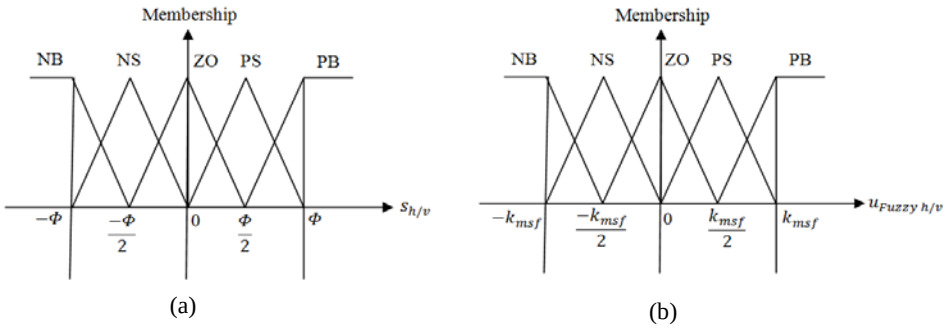

(a) (b)

Fig. 2. Fuzzy partition of the universe of discourse of : (a) $s_{h/v}$, (b) $u_{Fuzzy\ h/v}$

3.2. ACO-Based Parameters Tuning of the DFSMC

During the design, the parameters of the sliding surface (7) are relative to the performance of the control system. Hitting time, chattering phenomenon and speed of convergence are three important factors, which influence the performance of SMC. The parameter k_{msf} (see Fig.2) will influence how soon the state reaches to the sliding surface, the width of boundary layer will influence the chattering magnitude of SMC and the slope of the switching surface λ specifies the rate of convergence on the sliding surface. We will introduce an ACO algorithm to the problem of determining and optimizing these parameters of DFSMC for the TRMS. Generally, the advantages of ACO are their inherent parallelism, positive feedback accounts for rapid discovery of good solutions. In this paper, the Reference Based Error with Control Effort (RBECE) fitness function is chosen:

$$FF = \int (|e_h(t)| + |e_v(t)| + |u_h(t)| + |u_v(t)|)dt \qquad (22)$$

ACO is a one of the swarm intelligence techniques inspired by the foraging behavior of ant colonies [4]. By marking the paths they have followed with chemical substances called "pheromones" ants are able to communicate indirectly and find the shortest paths between their nests and a food places. When adapting this exploration /exploitation behavior of ants to solve discrete combinatorial optimization problems, artificial ants are considered a perfect research mechanism to discover the decision variable space of all possible solutions.

The search process of the ACO begins by choice of arbitrary solutions in decision variable space of the problem. During the tuning process, all ants of the colony deposit a uniformly distributed quantity of pheromone on the components of hopeful solutions. In this way, the global configuration of a decision space is iteratively changed and the ACO search is gradually oriented towards more desirable areas of the objective function space, where optimal or near-optimal solutions can be found. Consequently, ACO is used to find appropriate values of the $FSMC_{h/v}$ parameters $\Phi_{h/v}$, $k_{msf\ v/h}$ and $\lambda_{h/v}$.

We can represent the set of all parameters to be optimized by ACO in this problem with a vector F given as follows:

$$F = [\Phi_h \quad \Phi_v \quad k_{msfh} \; k_{msfv} \; \lambda_h \; \lambda_v] = [\quad^{i}\quad] \qquad (23)$$

With i=1…N, where N is the total number of the DFSMC parameters to be optimized; in our case N=6 parameters.

Each $FSMC_{h/v}$ (for the HS or for the VS) has three parameters to be optimized, there are basically six parameters. For each parameter, a set of a candidate values is given. To simplify, these purposed values are uniformly distributed on a limited interval using the following formulas.

Lets F^{i}_{min} and F^{i}_{max} be the bounds of i^{th} element in the vector F. So, we can obtain:

$$F_1^i = F_{min}^i,\ F_2^i = F_1^i + \frac{F_{max}^i - F_{min}^i}{J},\ldots\ldots,\ F_l^i = F_{max}^i \qquad (24)$$

The limit values F^i_{min} and F^i_{max} of each parameter are given in Table 1.

This subdivision method allows us to assign *J* candidate values for each parameter of the vector F then each parameter can be represented as a vector of *J* elements. The graphical representation of this optimization problem is given in the Fig.3. So, the six sets of parameters are arranged in six column lists where each candidate value is represented by a node. The ant proceeds from its nest, moves to any node of the next column, and then reaches the food source, and this completes a tour.

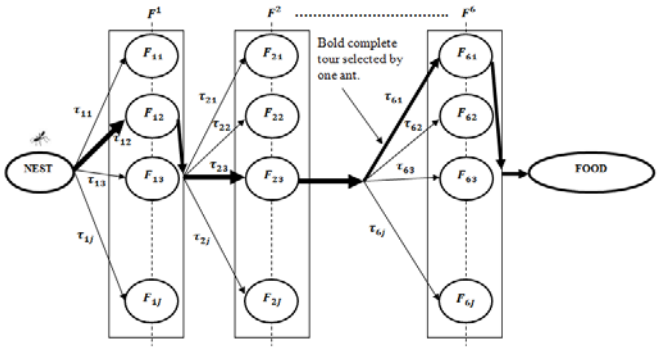

Fig. 3. Graphical representation of the optimization problem by ACO

After a full tour, each ant completes the selection of six parameters that will be tested later using the fitness function (22).

Starting from the initial state, i.e., the nest, an ant *k* with *k*=1…m, moves through the columns and stops at one of the nodes for variable F^6. For each variable, the node visited by the ant *k* is selected. In the Fig. 3, the generated path by ant *k* is marked by a bold fat line which associated the selected six candidate values. The selection of each candidate value is partially based on pheromone trails τ_{ij} between columns using the transition rule (25), where i=1…N and *j*=1…*J*, the size of the pheromone matrix in this case is N×*J*.

$$j = \begin{cases} \arg max_{y \in J} \{\tau_{iy}(t)\} & if\ r \le r_0 \\ j_1 & if\ not \end{cases} \qquad (25)$$

The selection may also be partially based on value of a random variable *r* uniformly distributed over the interval [0 1], after all ants have completed their tours at iteration *t* this variable should be incremented with the value $1–r_0/iter$ where *iter* represents the total number of iterations, r_0 is the initial value of *r*. The objective of this increment operation is to limit the choices to the best parameters characterized by a condensed pheromone trails. In (25) j_1 is selected based on a uniform probabilistic

rule over the candidate list {1,2,3,…,*J*}, the orientation to this choice is depends on the heuristic value of the parameter *r*.
At each iteration *t* where $0 \le t \le iter$ the ant *k* follows the trajectory which depends on the transition rule (25), this road represents the vector $F=[F^i]$of the parameters (nodes) selected by this ant. The solution obtained by this ant will be evaluated through the fitness function $FF(F^i_k)$.

The operation of updating the paths produced by each ant can be modeled by the following equation:

$$\tau_{ij}(t+1) = (1-\delta)\tau_{ij}(t) + \frac{Q}{FF\left(F_k^i\right)} \qquad (26)$$

Where: $\delta \in [01]$ represents the evaporation rate value of the pheromone trail and *Q* is a fixed positive parameter which define the amount portion of the pheromone update. Only the best tour will receive the uppermost pheromone concentration, as $FF(F^i_k)$ is small more the pheromone concentration is big.

The bloc diagram of ACO based- DFSMC for the TRMS is shown in Fig. 4.

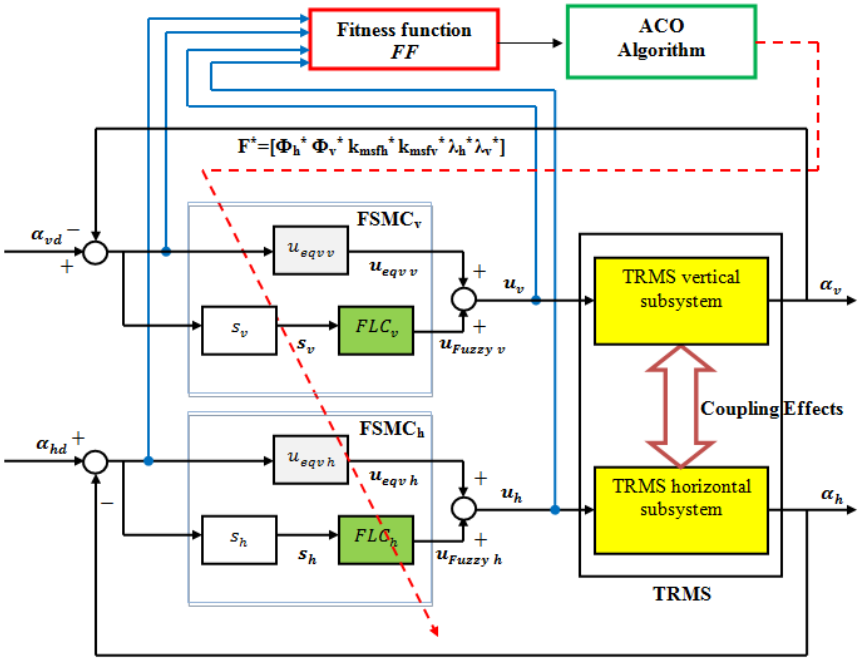

Fig. 4. Block diagram of ACO based-DFSMC for the TRMS

4. Simulation results

The control objective is to force the yaw angle α_h and the pitch angle α_v to follow a given reference trajectory α_{hd} and α_{vd} respectively. In order to control TRMS to track a specified trajectory quickly and accurately, the parameters of FSMC (HS and VS) controllers are tuned using the ACO algorithm. Simulations of tracking control with sine wave in horizontal and vertical planes are shown in Fig. 5 (a) and Fig. 5 (b). Amplitude and frequency of the desired sine wave trajectories imposed to the vertical and horizontal subsystems are set to 0.3 rad and 1/30 Hz respectively. The control signals u_v and u_h and the tracking errors e_v and e_h are also illustrated in Fig. 6 and Fig.7 respectively. Fig. 8 illustrates the best cost function evolution in term of the number of iterations, the final value of this function to which converge this algorithm is 0.4951.

The coefficients of ACO algorithm are chosen as follows: for each parameter, the number of candidate values J is set to 200, the number of ants is 10, tunable parameter r_0 is 0.3 and pheromone decay coefficient Q is set to 0.1, the parameter δ is set to 0.01. Initially, all tracks in the graph have been initialized with random pheromone concentrations τ_0, so $\tau_{ij}= \tau_0=0.1\times rand(N,J)$. In addition, this algorithm is run five times for 50 iterations, at each time the algorithm converges to an acceptable solution in less than 25 iterations. The learned parameters values are given in Table 2.

Table 1. Limit values of the parameters to be optimized

Parameter	Min	Max
Φ_h and Φ_v	1.5	120
$k_{msf\,h}$ and $k_{msf\,v}$	1.5	20
λ_h and λ_v	7	24

Table 2. Learned parameters values

Parameter	Final learned value
Φ_h	81.2940
Φ_v	108.6859
$k_{msf\,h}$	2.4296
$k_{msf\,v}$	10.1457
λ_h	11.9548
λ_v	13.3216

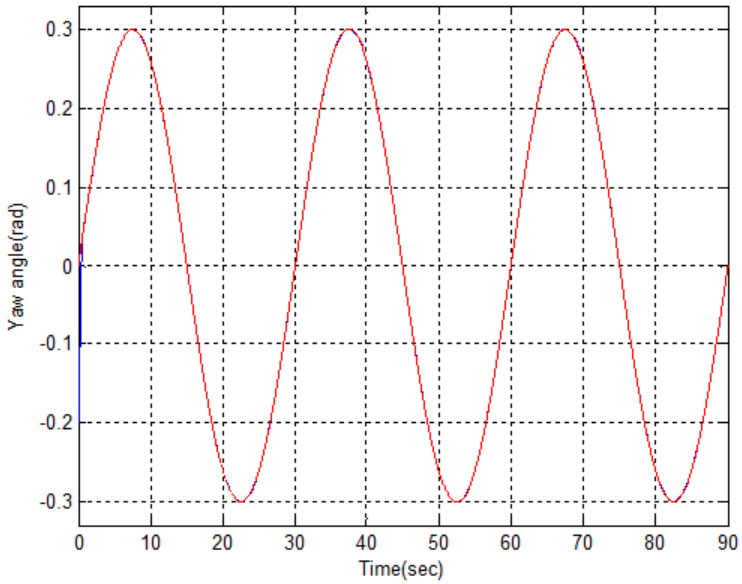

(a)

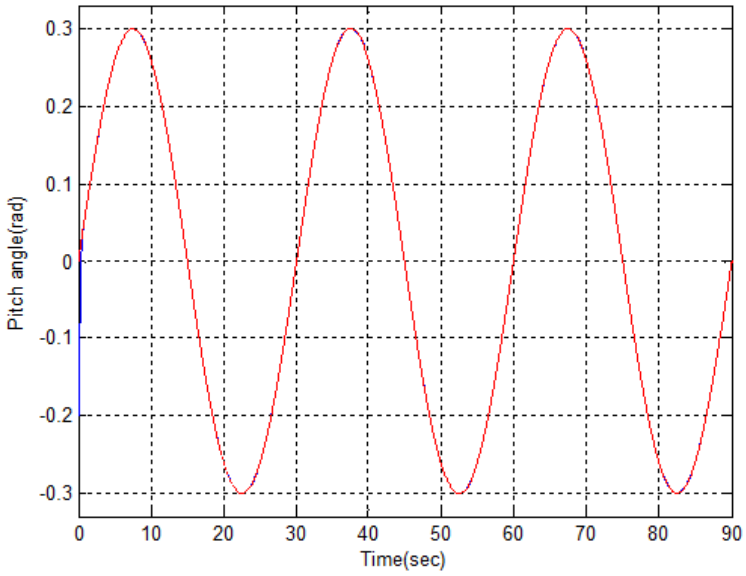

(b)

Fig. 5. (a)Yaw angle α_h, (b) the pitch angle α_v responses of the TRMS with DFSMC after optimization

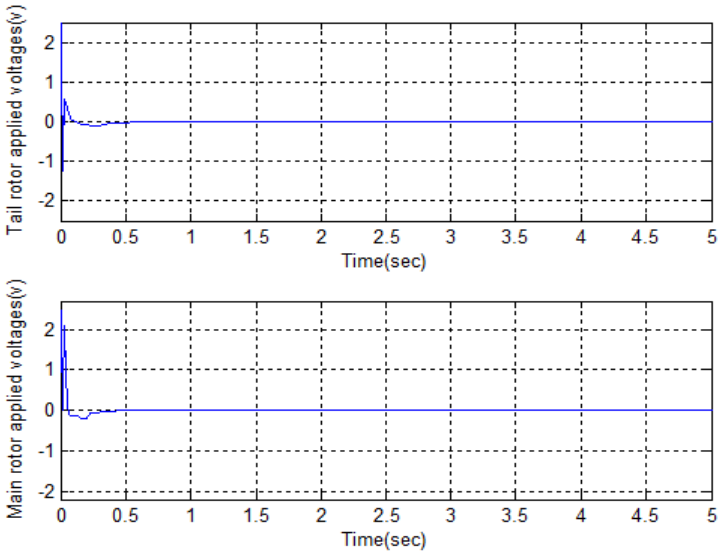

Fig. 6. Tail and main rotor applied voltages u_h and u_v obtained with DFSMC after optimization

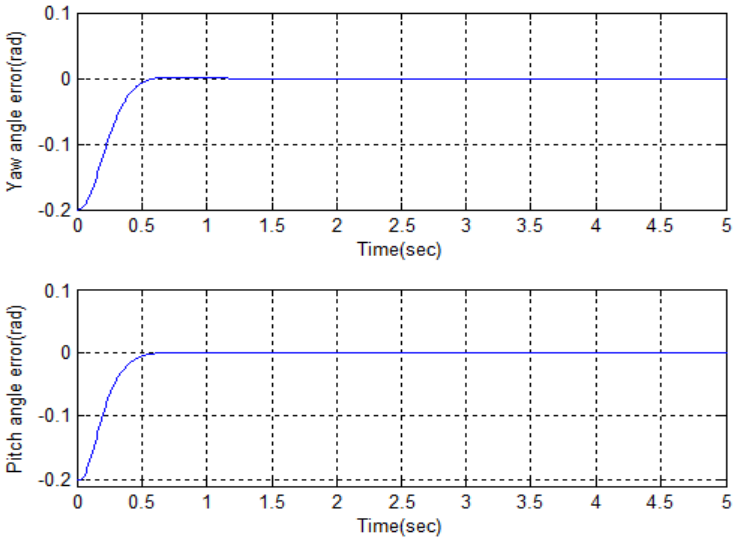

Fig. 7. Yaw angle error and pitch angle error

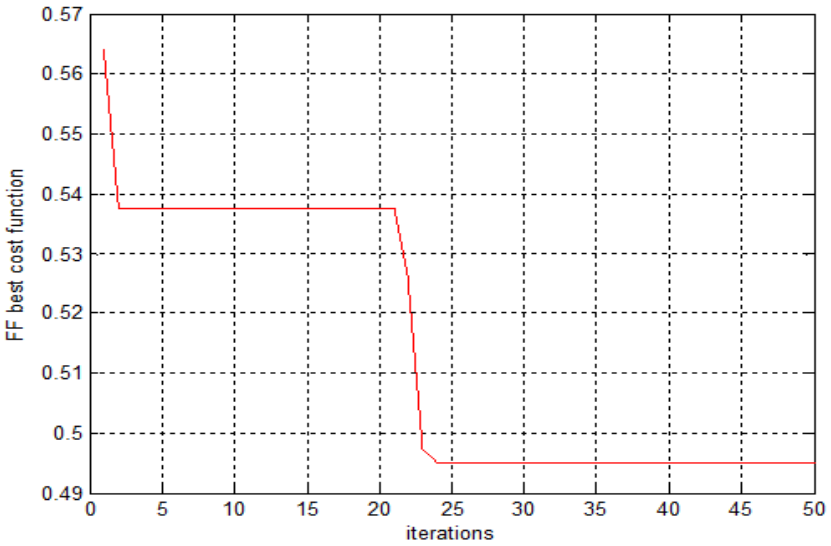

Fig. 8. Best value of the FF cost function in successive iterations

The simulations results obtained with a PID tuned with ACO (ACO-PID) are illustrated in the Fig. 9 (a), Fig. 9 (b) and Fig. 10 respectively. In order to show the differences between the DFSMC tuned with ACO controller (ACO-DFSMC) and the PID controller tuned with the same method and compare their performances. The optimization conditions for both ACO-DFSMC and ACO-PID controller should be same for accurate comparison, except that the MRSE cost function is multiplied by 0.001.

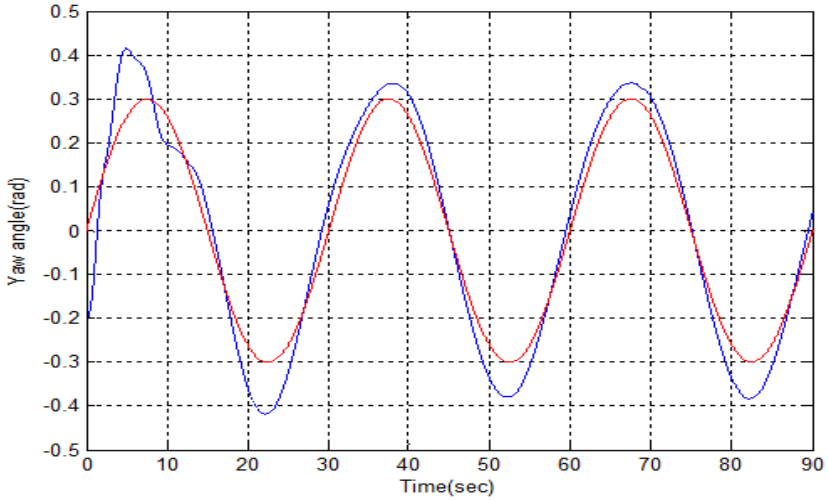

(a)

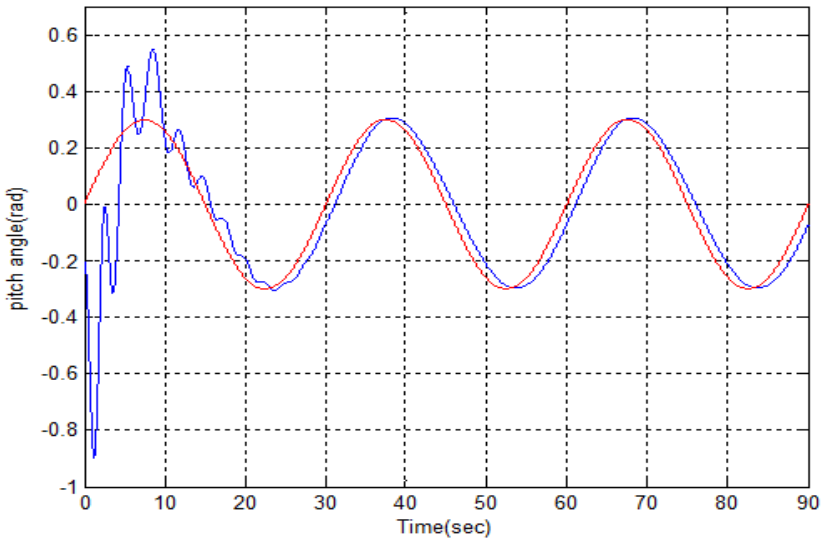

(b)

Fig. 9. (a) Yaw angle α_h, (b) pitch angle α_v responses of the TRMS with PID controller after optimization

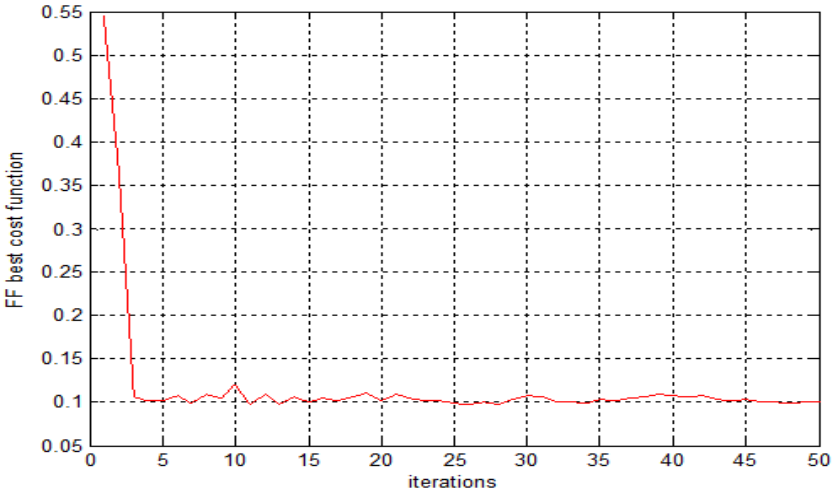

Fig. 10. Best values of the FF cost function in successive iterations (PID case)

The initial states of HS and VS systems are set to be $x_0=[\alpha_{h0}, \alpha_{v0}] = [-0.2(\text{rad}), \alpha_{v0}=-0.2(\text{rad})]$. Fig.4 (a) indicates the responses of the TRMS with the DFSMC after optimization using the ACO, it can be seen from these results that, the responses of the two subsystems (HS and VS) have no overshoot and they have quickly converges to their desired positions. The results of function optimization RBECE show that the basic ACO algorithm has good searching ability. It can be said also that the designed ACO-DFSMC gives better performance than using the PID controller designed by the same method under the same conditions, in term of convergence, response time, tracking error and control energy. Simulation results demonstrate that the ACO-DFSMC proposed obtains good performance. It also show that the method proposed eliminates chattering effectively and can guarantee the response speed and accuracy.

6. Conclusions

This paper introduces the ACO based tuning method for DFSMC to control the given TRMS trajectory. All membership functions parameters concerning the fuzzy controllers, and the sliding surface positives constants were determined using ACO algorithm. Also, robustness of the designed controller was tested in tracking of the sine wave trajectories. As a result, the DFSMC designed using ACO can achieve good accuracy in terms of trajectory tracking compared to the PID controller tuned with the same method. It is verified that is has better control performance in TRMS trajectory control. The obtained results are very encouraging and deserve to be implemented on the TRMS real system.

References

1. Boubakir, A., Boudjema, F., Boubakir, C. and Labiod, S.: A fuzzy sliding mode controller using nonlinear sliding surface applied to the coupled tanks system. Int. J. of fuzzy systems (2008)10(2), 112–118
2. Boubakir, A., Boudjema, F. and Labiod, S.: A neuro-fuzzy-sliding mode controller using nonlinear sliding surface applied to the coupled tanks system. Int. J. of automation and computing. (2009) 06 (1), 72–80
3. Yeh, F.K., Chen, C.M. and Huang, J.J.: Fuzzy sliding-mode control for a Mini-UAV. In: IEEE international symposium on Computational Intelligence in Scheduling, (2010) 3317–3323
4. M. Dorigo, V. Maniezzo and A. Colorni.: Ant system: Optimization by a colony of cooperating agents. IEEE Trans. Syst., Man, Cybern. B, Cybern, vol. 26 (1), (1996) 29–41
5. Feedback Co.: Twin Rotor MIMO System 33-220 user manual, 3–000 M5 (2008)
6. Juang, J.G., Liu, W.K. and Tsai, C.Y.: Intelligent control scheme for twin rotor MIMO system. In: IEEE International conference on mechatronics, (2005)102–107
7. Rahideh, A., and Shaheed, M.H.: Hybrid Fuzzy-PID-based Control of a Twin Rotor MIMO System. In: IEEE 32nd annual conference on industrial electronics, (2006) 48–53

8. Utkin, V.I.: Variable structure systems with sliding modes. Transactions of IEEE on Automatic Control (1977) (22), 212 – 222
9. Ramirez, S.H., Santiago, O.L.: Dynamical discontinuous feedback strategies in the regulation of nonlinear chemical processes. IEEE Transactions on Control Systems Technology, (1994) 2(1), 11 – 21
10. Slotine, J.J., Li, W.: Applied nonlinear control. Prentice-Hall, New Jersey (1991)
11. Slotine, J.J.,: Sliding controller design for nonlinear systems. International Journal of control (1984) 40 (2), 421–434
12. S. W. Kim, J. J. Lee.: Design of a Fuzzy Controller with Fuzzy Sliding Surface. Fuzzy Sets and Systems, (1995) 71(3), 359 – 367